Nondestructive measurement of charged particles by laser diffraction readout

Kensuke Homma

Physical Science, Graduate School of Science, Hiroshima University
Kagamayama 1-3-1, Higashi-hiroshima, Hiroshima, Japan
homma@hepl.hiroshima-u.ac.jp

Abstract

By utilizing macroscopic processes such as polarizations in an electro-optical(EO) crystal, a quasi nondestructive detection of charged particles can be achieved with the necessary energy consumption well below 1eV. EO crystals can convert electric fields to refractive index variations and the detection of the phase retardation of transmitted laser lights in a crystal makes the remote sensing possible. Diffraction patterns of the transmitted lights by a lens can be used to extract the extremely small phase retardation. A test experiment to verify the method has been performed using a thin direct current electron beam of 1nA by locating the beam at $\sim 300\mu$m from the crystal surface. The change of the diffraction pattern at the focal plane was observed associated with the existence of the remote electron beam.

1. Introduction

The detection principle of charged particles developed so far is based on the local inelastic processes such as ionizations and excitations with the energy consumption above the order of 1eV. However, if one could utilize more macroscopic processes such as polarizations in an electro-optical(EO) crystal for the electric field sensing, the necessary energy consumption is expected to be well below 1eV. This opens up new applications for quasi-nondestructive measurements especially for slow charged particles in addition to the application for the beam diagnosis of relativistic charged particles in accelerators. The novel detection method which remotely senses electric fields from charged particles has been demonstrated, where relativistic short electron bunches of 40ps containing 10^9 electrons per bunch were measured [1]. The principle is to measure instantaneous changes of the refractive index by electric fields of passing electrons by sensing the optical phase retardation *i.e.* changes of polarization states of transmitted laser lights in a crystal. The used crystal is $LiNbO_3$ which has the EO property (Pockels effect) originating from the uniaxial structure. However, there is no precedent to succeed to measure single charged particle based on the principle. Toward the ultimate goal, one has to develop a method to extract the extremely small phase retardation's as well as seeking for crystals with much larger EO coefficients than $LiNbO_3$. For the detection of the macroscopic polarizations caused by remote electric fields of charged particles, laser lights transmitted by an EO crystal with the local refractive index changes can be diffracted and interfered by a lens and the change of the diffraction pattern at the focal plane can be utilized to sense the extremely small refractive index changes. In the following sections, we would like to present results from a test experiment to verify the laser diffraction readout in a static condition using a weak thin direct current electron beam and a CW laser.

2. Principle of laser diffraction readout

Consider the case where a charged particle is moving along the x-axis and scanning lights are used to sense phase variations in an electro-optical crystal, transmitted along the z-axis, as illustrated in Fig. 1. The phase variation $\delta\Gamma$ induced by the charged particle moving at a distance R from the surface of the electro-optical crystal can be expressed as [1]:

$$\delta\Gamma = \frac{2\pi}{\lambda}\cdot\delta n\cdot\delta l = \frac{2\pi}{\lambda}\cdot f(r_{EO})E_T\cdot\frac{c}{n_L}\Delta t = \frac{f(r_{EO})}{2n_L n^2\epsilon_0}\frac{e}{\lambda\beta R}, \quad (1)$$

where λ is the wave length of the scanning light, δn is the refractive index variation by the transverse electric field E_T, $f(r_{EO})$ is a function of EO coefficients depending on the choice of a crystal and locations of the crystal with respect to the electric field, δl is the length of the variation along the laser light path, n_L is the refractive index for the path, c

is the speed of light, γ is the Lorentz factor, β is the relative velocity to c, Δt is approximated as $R/\gamma\beta c$, e is electric charge, and $n^2\epsilon_0$ corresponds to the dielectric constant of the crystal to E_T. Eq.(1) implies that the impulse due to an electric field becomes larger for a slower charged particle and hence applies more strongly to slower charged particles than to relativistic ones in the weak current limit.

The transmitted lights are further diffracted and interfered by a lens at the focal plane which produces the Fourier image of the original refractive medium shape in the crystal. In the case of the line shape expected from the trajectory produced by charged particles on the crystal surface, the Fourier image tends to extend to the outer region with the orthogonal rotation of the original line shape (see Fig. 2), while Gaussian profile of the incident laser light keeps a Gaussian shape with a smaller waist at the focal point if no phase variation exists. Therefore by sampling the diffraction pattern far from the focal point, one can improve the signal-to-noise ratio drastically to extract the extremely small phase variation.

3. Experiment with $LiNbO_3$ and results

We performed a test experiment with the $LiNbO_3$ crystal based on the configuration in Fig. 1. The direct current electron beam was used as a quasi-static charged particle source. The change of the refractive index was read out by the diffraction pattern at the focal plane by using the Nd:YAG CW laser and the image was further transfered to a wide dynamic range CMOS camera located outside the vacuum chamber via a flexible optical fiber bundle located inside the chamber. The flexible bundle is originally designed for endoscopes. Details of the parameters for the electron beam, the CW laser and the wide dynamic range CMOS camera are summarized in Tab. 1.

Suppose that the x, y and z-axis in Fig. 1 coincide with the crystal axis of $LiNbO_3$ respectively. The index ellipsoid of the crystal is expressed as (see [2] for instance):

$$\left(\frac{1}{n_o^2} - r_{22}E_2 + r_{13}E_3\right)x^2 + \left(\frac{1}{n_o^2} + r_{22}E_2 + r_{13}E_3\right)y^2 + \left(\frac{1}{n_e^2} + r_{33}E_3\right)z^2 + 2r_{42}E_2yz + 2r_{42}E_1zx - - 2r_{22}E_1xy = 1, \quad (2)$$

where $n_o = 2.286$, $n_e = 2.200$, r_{ij} are EO coefficients and E_j are the electric field components ($j = 1, 2, 3$ correspond to x, y, z respectively). Taking the symmetry of the electric field into account, the effect of E_1 and E_2 are canceled out, and the relevant field component becomes only E_3 in the case of Fig. 1. Hence in the case where linearly polarized laser lights propagate along the z-axis, the variation of the refractive index δn is expressed as:

$$\delta n = f(r_{EO})E_z = \frac{1}{\sqrt{n_o^2}} - \frac{1}{\sqrt{n_o^2 + r_{13}E_z}} \sim \frac{1}{2}n_o^{-3}r_{13}E_z \quad (3)$$

where $r_{13} = 8.6$pm/V and the polarization plane can take any directions in the $x-y$ plane. Fig. 2 shows the expected numbers of laser photons per CMOS pixel along the y-axis based on a semi-analytic calculation [3], when the beam trajectory is just on the x-axis as shown in Fig. 1. The tail portion of the Fourier image at the focal plane was sampled by locating the flexible optical fiber bundle underneath the focal point along the y-axis. The sampling was made so that the vicinity of the focal point can be pointed in the image, since the flexible fiber bundle itself rotates while the image is transfered.

100 shots were taken by the camera alternatively in the electron beam off (background) and on (signal) conditions. In total 400 shots were taken within 5 minutes by fixing the electron beam and the laser conditions and analyzed as follows. Fig. 3 shows randomly selected one shot without the electron beam, which indicates the direction of the focal point in the image along the intensity gradient of photons per pixel. Fig. 4 shows a subtracted profile between a pair of randomly selected background shots which indicates the laser intensity fluctuations in the most intense part even without phase variations. Fig. 5 shows a subtracted profile (signal - background) between a pair of randomly selected signal and background shots, which indicates the increase of the photon intensity in the opposite direction to the focal point. This is a signature of the phase variations expected in Fig. 2, whose typical pattern can be confirmed in any combinations of other arbitrary shots. The photon intensity per pixel is higher than what is expected in the ideal calculation as shown in Fig. 2. At present it is still difficult to discuss the diffraction pattern quantitatively, since the location of the fiber bundle is not accurately controlled yet in addition to the ambiguity of the absolute photon yield per resolution of the camera, and also the coupling of the fiber bundle to the camera is not satisfactory.

4. Summary and Future Prospects

The increase of the photon intensity at the focal plane expected from the phase variation due to electric fields by the direct current electron beam was verified which is qualitatively consistent with the characteristic pattern of the diffraction. By controlling the location of the optical fiber bundle and the coupling to the camera, we would be able to discuss the consistency between the observed diffraction pattern and the expectation. As a future prospect toward single charged particle detection, we have already found a good candidate, DKDP crystal whose EO coefficient is $\sim 10^3$ times larger than $LiNbO_3$ at the structural phase transition temperature of the crystal [4]. By using DKDP with the laser diffraction readout tested here, it is possible to achieve the nondestructive measurement of single charged particle based on the numerical calculation [3]. It is awaited for the moment to be confirmed experimentally.

References

[1] Semertzidis, Y. K. and others, Nucl. Instr. and Meth. A 452 (2000) 396-400.

[2] Amnon Yariv, Optical Electronics in Modern Communications, Oxford University Press, Inc., 1997, New York.

[3] K. Homma, in the process of the paper submission.

[4] A. S. Sonin, A. S. Vasilevskaya and B. A. Strukov, Soviet Physics - Solid State Vol.8 (1967) 2758-2760.

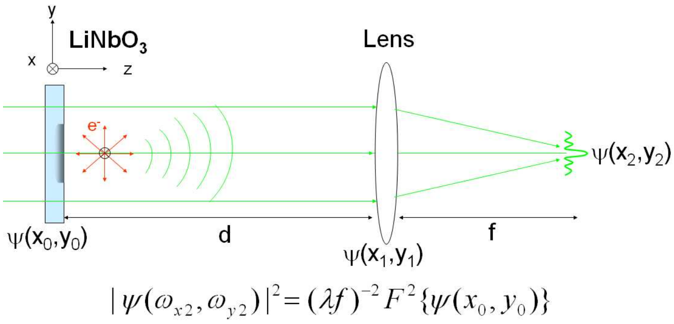

Fig. 1. Principle of the laser diffraction readout. The electric field of the charged particle beam along the x-axis induces refractive index variations on the surface of LiNbO$_3$. The laser lights transmitted by the crystal including the refractive index variations are diffracted and interfered by a lens at the focal plane. The lens effect corresponds to the Fourier transformation of the original refractive medium shape, $\Psi(x_0, y_0)$, where ω_{x_1} and ω_{y_2} correspond to $\frac{2\pi}{\lambda f}x_2$ and $\frac{2\pi}{\lambda f}y_2$ respectively.

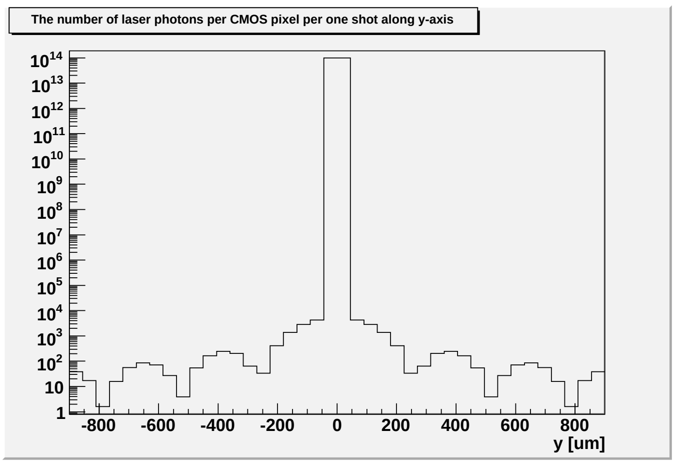

Fig. 2. The expected numbers of laser photons per CMOS pixel along the y-axis, when the beam trajectory is just on the x-axis as shown in Fig. 1.

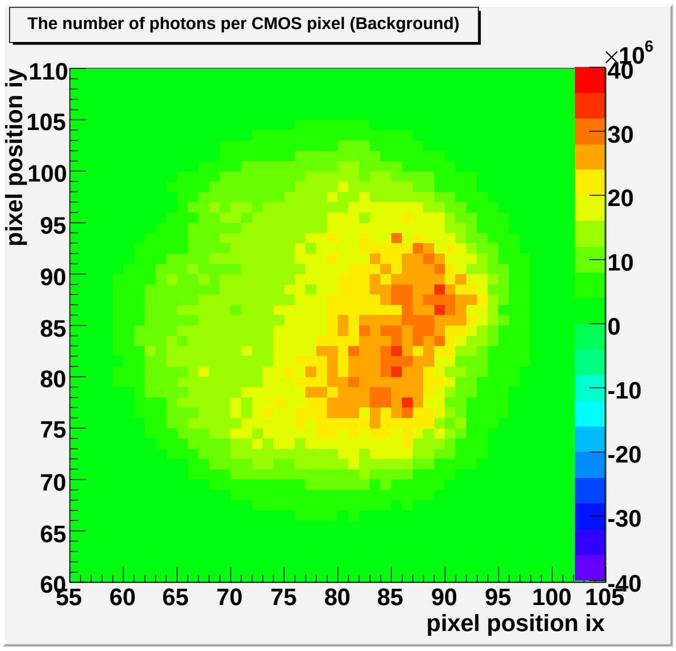

Fig. 3. Diffraction pattern in a shot without the electron beam.

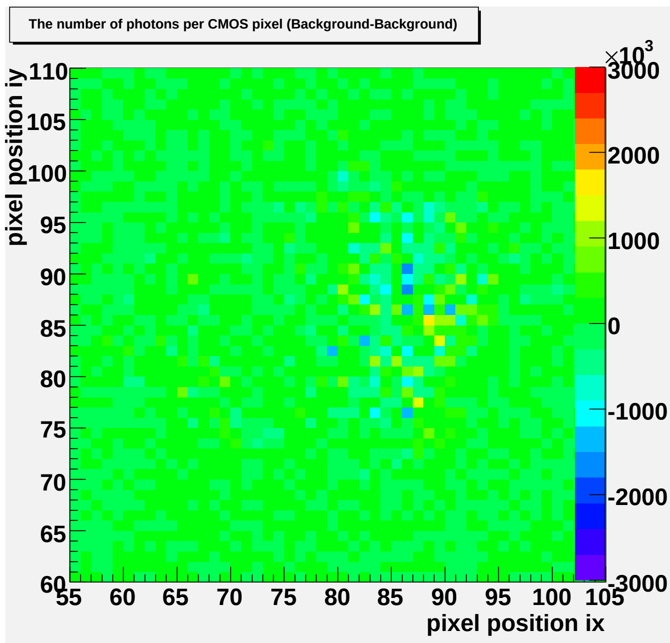

Fig. 4. Subtracted diffraction pattern between a pair of randomly selected background shots.

Table 1
Parameters used for Fig. 2.

One standard deviation of a laser profile	$\sigma = 1000\mu$m
Total intensity of a Gaussian laser beam	$I_0^2 = 10^{19}$ ($\sim$1W$\times$1sec)
Peak intensity of a Gaussian laser beam	$A_0^2 = \frac{I_0}{2\pi\sigma^2}$
Laser wave length	$\lambda = 0.532\mu$m
Focal length	$f = 100$mm
Electron beam diameter	50μm(FWHM)
Electron beam current	$\sim$ 1nA
Electron distance from the crystal surface	$R = 500\lambda$
Electron kinetic energy	$E_k = 4$keV
Electron velocity relative to light velocity	$\beta = 0.124$
Electro-optic coefficient of $LiNbO_3$	$r_{13} = 8.6$[pm/V]
Rectangle size with phase variations	5000μm $\times$ 204μm
The number of electrons during the effective impact time	$\sim$ 0.1
Local phase retardation	$\delta\Gamma = 1.76 \times 10^{-10}$
CMOS camera dynamic range	$\sim$17 bits
CMOS pixel size	45μm $\times$ 45μm
Exposure time	20μsec

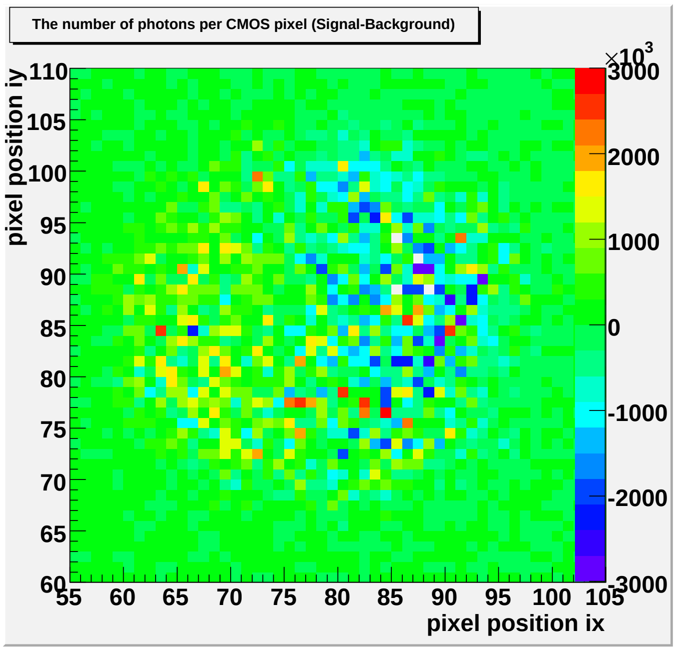

Fig. 5. Subtracted diffraction pattern(signal-background) between a pair of randomly selected signal and background shots.